LARGE EDDY SIMULATION OF A SUPERSONIC TURBULENT BOUNDARY LAYER AT M=2.25

Abdellah HADJADJ, Samuel DUBOS, Guillaume RIBERT

Institut National des Sciences Appliquées de Rouen, CORIA - Unité Mixte de Recherche C.N.R.S. 6614. Avenue de l'Université, 76801 Saint Etienne du Rouvray, France

Abstract. This work deals with numerical simulation of a spatially-developing supersonic turbulent boundary layer at a free-stream Mach number of $M = 2.25$ and a Reynolds number of $R_{e_\theta} = 5000$ with respect to free-stream quantities and momentum thickness at inflow. Since a shock-capturing scheme is used, a hybrid numerical scheme has been developed to reduce its dissipative properties. The issue of the generation of coherent turbulent boundary conditions is also addressed. A method originally developed by Lund, based on a rescaling technique, has been modified by adjusting the scaling coefficient to provide smooth transition between the inner and the outer parts of the boundary layer. This modification is essential for avoiding the drift previously observed in the mean streamwise velocity profile. The obtained results are analysed and discussed in terms of mean and turbulent quantities. Excellent agreement between LES, DNS and experimental data is obtained. The validity of the assumptions of the strong Reynolds analogy (SRA) is also addressed.

Key words: Unsteady turbulent supersonic flows, large eddy simulation, turbulent boundary conditions, strong Reynolds analogy, shock-capturing schemes.

1. Introduction

Eddy structures and internal dynamics of compressible supersonic turbulent boundary layers (see Fig. 1) may play an important role in aerospace applications, specifically when surface heat transfer on high-speed vehicles or unsteadiness in shock/turbulent boundary layer interactions are of concern. Today, large-eddy simulation has demonstrated its capabilities in calculations of relatively complex flows and can be used as a design tool for real-time optimization. The rising computational power and the improved numerical techniques are able to solve more scales presented in turbulent flows and thus predicting unsteady effects better than RANS or URANS methods. The purpose of this paper is to develop reliable CFD tools and estimate the area of their applicability for complex compressible flows situations, including shocks, boundary layer, acoustics, compressibility effects... The primary focus of the present contribution is the study of a spatially-developing turbulent boundary layer at Mach number 2.5 over an adiabatic flat plate using LES method. This test-case provides the (unsteady) inflow conditions to the shock-boundary layer interaction problem studied experimentally by Deleuze and Laurent [12, 13]. In addition, analyses of the turbulent structures may significantly contribute to the understanding of the turbulence behaviour of supersonic boundary layers as well as the development of improved compressible turbulence models.

Figure 1. Large eddy simulation of supersonic boundary layer. Three-dimensional instantaneous view of density [3].

2. Numerical procedure and LES methodology

In addition to sub-grid scales modeling, another issue of LES technique is the choice of the numerical method. As pointed out by Ghosal [1], Kravchenko and Moin [2], the truncation error of low-order schemes may exceed the SGS term, leading to a high numerical damping. Moreover, when fully compressible flows are investigated, pressure (or density) discontinuities may appear and have to be captured without adding too much numerical viscosity. To achieve this a fifth-order WENO scheme [4] combined with a centred fourth-order scheme is used to calculate the convective fluxes. Using a selective Ducros' sensor, it was possible to confine the use of the WENO scheme to the portions of the flow that contain discontinuities (shocks). This technique contributes to reduce significantly the dissipation of the numerical scheme. Viscous terms are discritized using a centred fourth-order accurate, while an explicit third-order Runge-Kutta of Shu and Osher [5] is used for time integration. For nu-

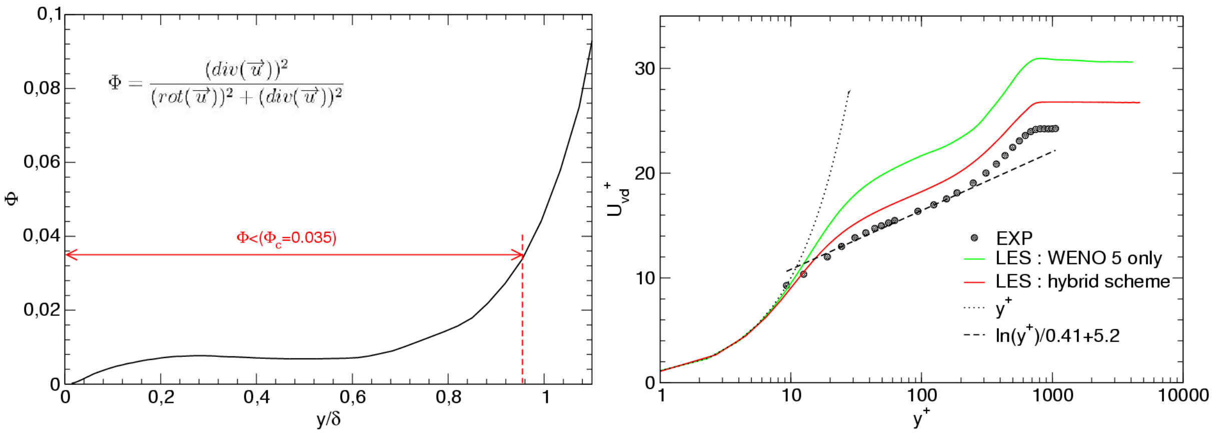

Figure 2. Mean distribution of Ducros' sensor in the boundary layer (left). Influence of numerical scheme on the longitudinal velocity profile (right).

merical stability reasons, the minimum value of Φ (where Φ is the Ducros' sensor defined in Fig. 2), for which the centred scheme is selected, is fixed to $\Phi_c = 0.035$.

The computed mean value of Φ shows that the centred scheme is mainly used within the boundary layer, since $\overline{\Phi} < \Phi_c$ for $y/\delta < 0.96$ (see Fig. 2 - left). The advantage of using a hybrid scheme is evident from Fig. 2 (right), where the normalised mean velocity profile U^+_{vd} (with $U^+_{vd} = \int_0^{U^+} \sqrt{\rho/\rho_p}\; dU^+(y^+) = ln(y^+)/\kappa + C$) exhibits a better behaviour. In particular, if only the WENO scheme is used, the value of the skin-friction velocity, u_τ, is underestimated by approximately 30% compared to experimental data. However, this value is reduced to ∼10% with the hybrid scheme. As previously reported [14, 15], this kind of underestimation is customary for compressible LES. Concerning the inflow boundary conditions, an existing method of generation of unsteady compressible turbulent boundary layers [9, 10, 11] has been modified to avoid the drift of the mean velocity profile, observed in supersonic boundary layer simulations. The modification was achieved through an appropriate adjustment of the scaling coefficient to provide smooth transition between the inner and the outer parts of the boundary layer [3]. Doing so, the new recycling and rescaling method becomes robust and relaxes faster towards the target experimental values (mainly the skin-friction velocity, $u_\tau = \tau_w^{1/2}$, where $\tau_w = \nu(\partial u/\partial y)|_w$ and the boundary-layer thickness δ). The main advantage of the recycling-rescaling method is to allow the simulation to generate its own inflow data with more computationally efficiency than the random fluctuation approach or the forced laminar-to-turbulent transition method.

3. Results and discussion

A supersonic incoming boundary layer at $M_\infty = 2.3$ and $R_{e_\theta} = 5000$ (in the absence of interacting shock) are reported here after. The size of the computational domain is: $L_x \approx 15\,\delta$, $L_y \approx 6.5\,\delta$ and $L_z \approx 0.6\,\delta$, where $\delta = 10.83\,mm$ is the incoming boundary-layer thinckness. Notice that the spanwise length of the computational domain represents $1/10^{th}$ of the experimental wind tunnel extent. The two-point autocorrelation coefficients in the homogeneous direction (z), for both the turbulent velocity and thermal variables, are examined. Results (not presented here for concision) show that the decorrelation of velocity fluctuations is achieved over a distance of $L_z/2$, indicating that the computational domain is chosen large enough to not inhibit the turbulence dynamics. The mesh has about 2.4×10^6 grid points, distributed in wall units as: $\Delta x^+ = 40$, $\Delta z^+ = 7$ and $\Delta y^+_{min} = 1$, where $y^+ = y u_\tau/\nu_w$, with ν_w and ρ_w the kinematic viscosity and the density at the wall, respectively. These computations were performed on a parallel IBM-SP Power4 using 40 processors and required 140h of CPU time.

3.1. Instantaneous structure and mean properties

An unsteady view of the supersonic flow is presented in Fig. 3. The examination of the instantaneous three-dimensional iso-vorticity field shows that the boundary layer is fully developed and self preserving.

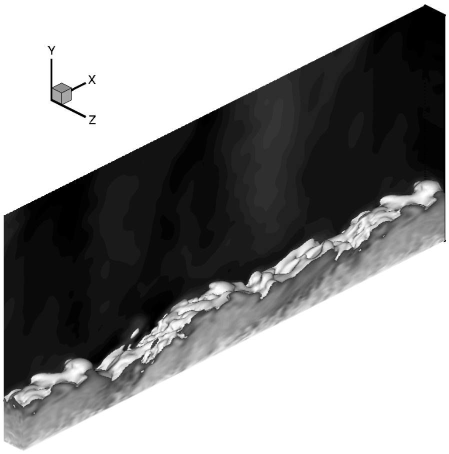

Figure 3. Numerical flow visualization. Instantaneous density field with iso-vorticity contours.

Also, the simulation reveals the appearance of large-scale motion in the outer region of the boundary layer, dominated by the entrainment process. These large-scale structures are particularly active near the boundary-layer edge, where they remain coherent long enough and are strongly responsible for the intermittency of the boundary layer its growth rate. Near-wall streaks can be visualized by contours of the streamwise velocity fluctuation, which is shown in Fig. 4 in a wall-parallel plane at $y^+ \sim 10$. It is obvious from Fig. 4 that the computational domain contains several streaks (more than 5) in the spanwise direction, spaced by about $L_z^+ = 455$ wall units, which is 4 times larger than the "Minimal Flow Unit"recommended by Jimenez & Moin [16].

Figure 4. Instantaneous longitudinal velocity fluctuations in a wall-parallel plane at $y^+ \approx 10$.

The reported turbulence statistics are examined to evaluate their consistency with both DNS [6] and experimental measurements [12, 13]. They are based on time-averaging of the instantaneous three-dimensional fields that were extracted from a time series covering 160 characteristic times $\tau_m = \delta_i/U_\infty$, where δ_i is the incoming boundary-layer thikness evolving at a free-stream velocity, U_∞. As shown in Figs. 5 and 6, simulations match well with experimental results (for other parameters of interest see the reference [3]).

3.2. Strong Reynolds Analogy

In supersonic turbulent flows, the Strong Reynolds Analogy (SRA) is derived from the assumptions that the total temperature fluctuations are negligible, and the Prandtl number is one, which leads to the following relation:

$$SRA = \frac{\sqrt{\overline{T'T'}}/\widetilde{T}}{(\gamma-1)\bar{M}^2\sqrt{\overline{u'u'}}/\widetilde{u}} \approx 1 \tag{1}$$

where $\bar{M} = \bar{u}/\bar{c}$ is the local Mach number. Relation (1) implies that velocity and temperature fluctuations are anti-correlated, i.e., their correlation coefficient is:

$$R_{u'T'} = \frac{\overline{u'T'}}{\sqrt{\overline{u'^2}\ \overline{T'^2}}} \approx -1 \tag{2}$$

As shown in Fig. 7 (left), the relation (1) is valid in the whole boundary layer. However, the value of the measured correlation coefficient $-R_{u'T'}$ is less than unit

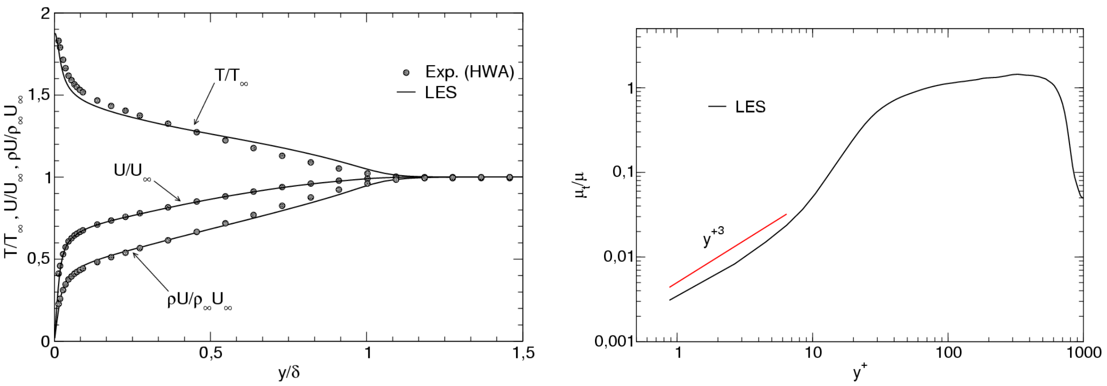

Figure 5. Distributions of normalized mean flow variables (left) and subgrid turbulent viscosity as function of wall-normal distance (right)

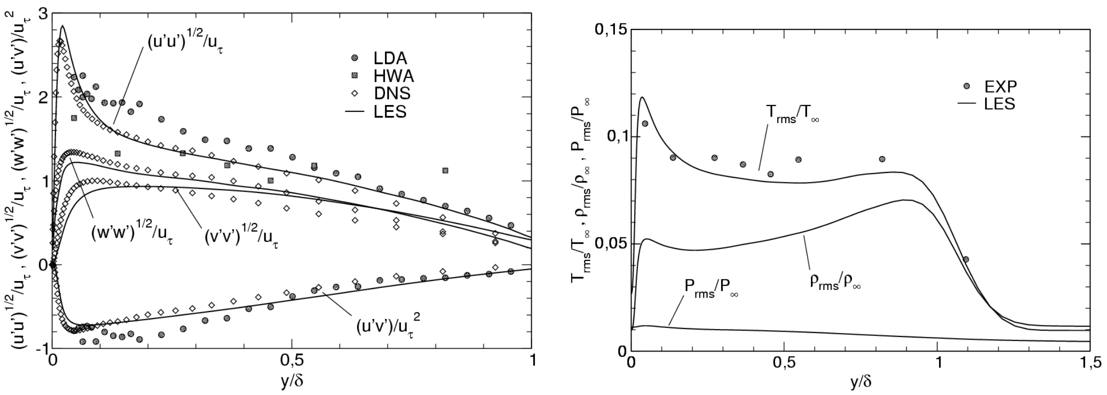

Figure 6. Distributions of normalized Reynolds shear stresses (left) and r.m.s values (right)

($\approx$ 0.85). In addition, recent DNS [6, 7] have shown that this coefficient fails to 0.60 throughout most of the boundary layer and exhibits a maximum value of 0.84 when the wall is approached. DNS and LES (performed in this study) reproduce the same trend, except in the outer part of the boundary layer where the correlation coefficient fall to 0.45 for LES. As suggested by Gaviglio [8], discrepancies observed between experiments and simulations may be due to a difference in the magnitude of the acoustic field which is much lower in the computations than in blowdown supersonic wind tunnels. Furthermore, this result confirms that the fluctuations of the total temperature are not negligible and the strong Reynolds analogy (SRA) is not valid.

4. Conclusions

In this paper, a new approach, based on the use of a combined filter and discontinuity sensor for monitoring the flow solution, is developed and validated for the simulation of supersonic turbulent flows containing shocks with fine scale flow structures. The current research is motivated by the desire to construct reliable compressible Navier-Stokes solvers with accurate numerical tools for predicting complex supersonic aerodynamics in real applications. The numerical procedure, developed in this study (a 3D compressible LES solver with improved inflow-data generation method)

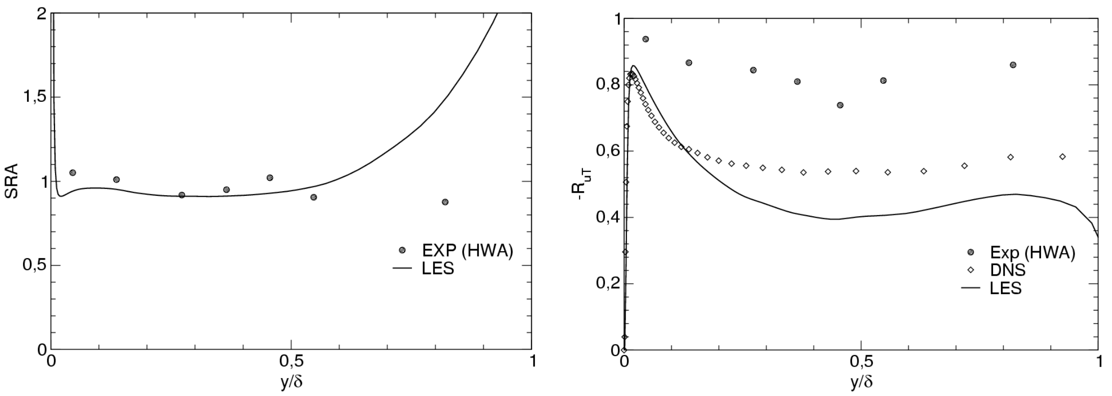

Figure 7. Plot of the the Strong Reynolds Analogy (left) and the $-R_{uT}$ correlation (right) versus y/δ.

has been used to analyse the spatial evolution of a supersonic turbulent boundary layer at M=2.25. This test-case provides the (unsteady) inflow conditions to the shock-boundary layer interaction problem studied experimentally by Deleuze and Laurent [12, 13]. Distributions of mean and turbulent flow quantities are analysed and compared to experimental measurements and DNS data. Very interesting results are obtained. In particular, it is found that the LES accurately predicts the mean temperature and density profiles, skin friction, root mean square of velocity, temperature fluctuations and Reynolds shear stress profiles. In agreement with DNS [6, 7], this study shows that the u velocity component and temperature are weakly anti-correlated ($-R_{uT}$ is approximately 0.5). Experimental evidence, however, suggests a higher value of the correlation coefficient than was found in this simulation. Finally, fluctuations of the total temperature are not negligible and the strong Reynolds analogy (SRA) is not valid.

Acknowledgements

Part of this work has been carried out within the research activities of the ATAC group (Aérodynamique des Tuyères et Arrière-Corps) supported by CNES and ONERA. Computational facilities were provided by CNRS - IDRIS (Institut du Développement et des Ressources en Informatique Scientifique, Paris) and CRIHAN (Center de Resources Informatiques de HAute Normandie, Rouen).

References

[1] Ghosal S. (1996) An analysis of numerical errors in large eddy simulations of turbulence, *J. Comp. Phys.* **125**: 187-206.

[2] Kravchenko A. G., Moin P. (1996) On the effect of numerical errors in large eddy simulations of turbulent flows, *J. Comp. Phys.* **131**: 310-322.

[3] Dubos S. (2005) Simulation des grandes échelles d'écoulements turbulents supersoniques, *Ph.D Thesis, INSA of Rouen.*

[4] Jiang G. S. and Shu C. W. (1996) Efficient implementation of weighted ENO schemes, *J. Comp. Phys.* **126**: 202-228.

[5] Shu C. W. and Osher S. (1988) Efficient implementation of essentially non-oscillatory shock capturing schemes, *J. Comp. Phys.* **77**: 439-471.

[6] Pirozzoli S., Grasso F. and Gatski T. B. (2004) Direct numerical simulation and analysis of a spatially evolving supersonic turbulent boundary layer at M=2.25, *Phys. Fluids* **16**: 530-545.

[7] Guarini S., Moser R., Shariff K. and Wray A. (2000) Direct numerical simulation of a supersonic turbulent boundary layer at Mach 2.5, *J. Fluid Mech.* **414**: 1-33.

[8] Gaviglio J. (1987) Reynolds analogies and experimental study of heat transfert in the supersonic boundary layer, *Int. J. Heat Mass Transfer* **30**: 911-926.

[9] Stolz S. and Adams N. A. (2003) Large-eddy simulation of high-Reynolds-number supersonic boundary layers using the approximate deconvolution model and a rescaling and recycling technique, *Phys. Fluids* **15**: 2398-2412.

[10] Urbin G. and Knight D. (1999) Compressible large eddy simulation using unstructured grid: supersonic boundary layer, *Second AFOSR Conference on DNS/LES, Kluwer Academic Publishers, June 7-9 Rutgers University*: 443-458.

[11] Lund T. S., Wu X. and Squires K. D. (1998) Generation of turbulent inflow data for spatially-developping boundary layer simulations, *J. Comput. Phys.* **140**: 233-258.

[12] Deleuze L. (1995) Structure d'une couche limite turbulente soumise à une onde de choc incidente, *Ph.D thesis, Université Aix-Marseille II, France.*

[13] Laurent H. (1996) Turbulence d'une interaction onde de choc/couche limite sur une paroi plane adiabatique ou chauffée, *Ph.D thesis, Université Aix-Marseille II, France.*

[14] Spyropoulos E. T. and Blaisdell G. A. (1998) Large-eddy simulation of a spatially evolving supersonic turbulent boundary-layer flow, *AIAA J.* **36**: 1983-1990.

[15] Sagaut P., Garnier E., Tromeur E., Larcheveque L., Labourasse E. (2004) Turbulent inflow conditions for large-eddy simulation of compressible wall-bounded flows, *AIAA J.* **42**: 469-477.

[16] Jimenéz J. and Moin P. (1991) The minimal flow unit in near-wall turbulence, *J. Fluid Mech.* **225**: 213-240.